https://erjm.journals.ekb.eg
ISSN: 1110-1180

DOI: ---------

ERJ
Engineering Research Journal
Faculty of Engineering
Menoufia University

# Structural Behavior of Ferrocement I -Beams with Web Openings Experimental Study

**Yousry B.I. Shaheen[1], Ghada M. Hekal [1*], Ayman M. Elshaboury [2]**

*[1]Civil Engineering Department, Faculty of Engineering, Menoufia University, Egypt.*
** Higher Institute of Engineering and Technology, Menoufia*
*[2]Ph.D. candidate, Civil Engineering Department, Menoufia University, Egypt*
*(Corresponding author: aymanelshaboury55@gmail.com)*

**ABSTRACT**
The main purpose of the current study is to investigate the effect of openings existence on the structural behavior of ferrocement I –beams with two different types of reinforcing metallic and non-metallic meshes. Eight beams are tested under a four-point loading system until failure. The beams are divided into two groups according to the type of meshes used as reinforcement. Each group contains a control I-beam with no openings and three beams with one, two, and three openings. To keep a constant reinforcement ratio, the two groups are, respectively, reinforced with three layers of welded steel meshes and two layers of tensar meshes. It was observed that beams reinforced with welded steel meshes showed a higher ultimate load, deflection, ductility ratio, and energy absorption compared to beams reinforced with tensar meshes. In addition, beams with three openings showed a lower ultimate load, deflection, ductility ratio, energy absorption, and load-to-weight ratio than the other beams with the same type of reinforcing meshes.

***Keywords:*** *Ferrocement; I-beams; welded mesh; tensar mesh; Openings.*

## 1-Introduction

Ferrocement is a relatively new cementitious composite that is strengthened with closely spaced layers of continuous and relatively thin wire mesh. P. L. Nervi, an Italian architect, invented ferrocement in 1940 [1, 2]. There are numerous advantages to ferrocement, including the availability of ferrocement raw materials in most countries, the ability to manufacture in various shapes, needless of high labor skills, and the ease of construction at a low cost. Ferrocement mainly consists of cement, sand, and water with the possibility of adding some chemical additives to reduce the interaction between the matrix and the galvanized reinforcement. Ferrocement may require some pozzolanic materials such as silica fume or fly ash to improve certain properties [3]. The behavior and mechanical properties of ferrocement have been studied in many research [4-10]. Previous research showed that ferrocement adapts slowly to increasing loads by increasing its extensibility, resulting in narrower crack widths that are lower than in reinforced concrete. The number of layers (volume fraction) of the wire mesh layers is usually directly related to the tensile strength of ferrocement. The studies observed that, where everything else is equal, the tensile strength at initial cracking in ferrocement was exactly proportional to the specific surface of reinforcement [11]. Based on previous researches, the compressive strength of ferrocement was equivalent to that of the mortar mix. Solid and hollow columns that were prophetically reinforced with wire mesh, on the other hand, showed dramatically increased strength [12, 13]. It has been found that, as compared to reinforced concrete, the crack width under working load in ferrocement tends to remain relatively small, resulting in good impermeability, stiffness, and durability [14, 15]. Regardless of the type and composition of mesh or mortar strength used, the shear strength of ferrocement was stated to be approximately equal to 32% of its equivalent bending strength [16]. Due to its stronger ability to absorb impact energy than ordinary reinforced concrete, ferrocement was particularly effective at resisting impacts, and the damage was localized at the impact zone [17]. Some complementary works in construction, such as electricity, telephony, water supply, and air conditioning, require special openings, especially in beams, therefore; this study is been conducted to investigate the effect of openings on the structural behavior of ferrocement I –beams with two types of reinforcing meshes [18]. It is clear that by adding openings in beams, the strength of beams decreased depending on the opening position, dimensions, and the number of openings. According to ACMA (2014), a ferrocement I-beam was constructed by bolting two ferrocement Channel-beams back-to-back that is reinforced with two, four, and six welded wire mesh. The study's findings revealed good flexural strength performance, but the beam did not achieve the ductility behavior predicted in reinforced concrete

beams [19]. To the authors' knowledge, there is not much research that has discussed the effect of web openings on the behavior of the ferrocement I-beams. Therefore, the current paper may be considered as a required study that can be added to the previous research.

**2-Experimental Program**

Eight beams were cast and tested to study their behavior under flexural loadings. The tested beams were grouped into two groups according to the type of reinforcing mesh used. The details of the two groups are listed in Table 1.

**Table 1: Details of the tested beams.**

| Group No. | Code of beam | Meshes used | No. of Openings | Vol. Fraction % |
|---|---|---|---|---|
| A | W0 control | Three layers of welded steel mesh | - | 0.327 |
| | W1 | | 1 | |
| | W2 | | 2 | |
| | W3 | | 3 | |
| B | T0 control | Two layers of tensar mesh (Type SS40) | - | 2.530 |
| | T 1 | | 1 | |
| | T 2 | | 2 | |
| | T 3 | | 3 | |

To generate flowable mortar that can be cast easily into the molds without generating honeycombing, the coarse aggregate was not included in the mortar. Natural siliceous sand was used as a fine aggregate in the experiment. The sand properties meet the requirements of E.S.S. 1109/2008 [20]. The sand was pure and practically impurity-free, with a specific gravity of 2.6 and a modulus of fineness of 2.7. The cement used was Blast furnace Cement from Assiut Cement Company. The cement used complied with Egyptian Standard Specification E.S.S. 4756 -1/2013 [21]. To improve the strength and permeability of the mortar matrix, Silica Fume (S.F.) and fly ash were utilized as a partial replacement of cement by weight. Polypropylene mesh e 300 was also utilized to improve the concrete properties. The ferrocement beams were mixed and cured with pure drinking fresh water that was free of pollutants. A superplasticizer was used to increase the workability and make the casting process easier. Normal mild steel bars with a diameter of 6 mm and yield strength of 240 MPa were used. Several types of reinforcing steel meshes were used as demonstrated in figure (1). The ferrocement beams in group A were reinforced with welded steel mesh.

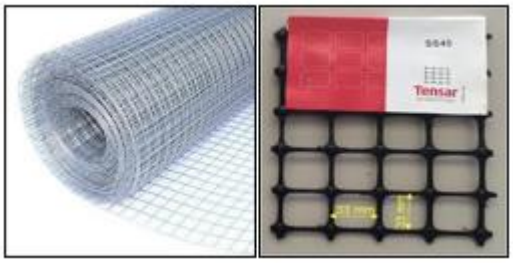


Welded mesh tensar mesh

**Figure 1: The types of meshes used.**

Table (2) shows the technical specifications and mechanical properties of welded steel mesh according to Shaheen et al. (2021) [22]. Tensar mesh type SS40 was used as reinforcement for group B to invistigate the effect of non-metallic mesh on the behavior of ferrocement I-beams compared with a metallic mesh having a constant reinforcing ratio. Tensar is a monolithic geogrid with inherent joints that is rigid and durable. They are oriented in two directions, resulting in ribs with a high degree of molecular orientation that extends across the whole node region. The ribs are rectangular and have square edges. Table (2) lists the technical specifications and mechanical properties of tensar mesh type SS40 as provided by the manufacturer [23].

**Table 2: Technical specifications and mechanical properties of welded metal mesh and tensar mesh.**

| Welded Metal Mesh [22] | | Tensar Mesh [23] | |
|---|---|---|---|
| **Dimensions Size** | 12.5×12.5 mm | **Dimensions Size** | 33 × 33 mm |
| **Weight** | 430 gm/m$^2$ | **Weight** | 530 gm/m$^2$ |
| **Diameter** | 0.8 mm | **Thickness** | 2.8 mm |
| **Modulus of elasticity** | 170000 MPa | **Modulus of Elasticity** | 100000 MPa |
| **Poisson's ratio** | 0.28 | **Poisson's ratio** | 0.3 |
| **Proof Stress** | 400 MPa | **Proof Stress** | 198 MPa |

The tested beams had fixed dimensions of 2200 mm in length, flange dimensions of 200 mm in width and 40 mm thickness, web dimensions of 170 mm in height and 30 mm in thickness, thus the total height of the sample is 250 mm. The locations of openings were chosen in the predicted critical shear zone as well as in the predicted critical moment, and shear zones together. On another side, the opening area was chosen so that it would not be large enough to affect the efficiency of the beam, and at the same time allow the passage of the necessary cables. The distance between the two substrates was 2000 mm, and tested beams were loaded under four-point loadings until failure. Figure (2) shows the dimensions of the tested beams while the shape of the used meshes during its preparation and until the full casting is shown in figure (3). The type of

mesh utilized and the number of openings was the two key variables investigated. During the test, the vertical displacement versus the load was recorded. The control station, loading cells, and testing frame were all parts of the testing facility. For all of the test specimens, the load was applied in increments of 5.0 to 20 kN. At all stages of loading, all deformation characteristics and cracking patterns were comprehensively measured. The experimental program carried out in this study was performed in the laboratory of testing building materials at the Faculty of Engineering - Menoufia University - Egypt.

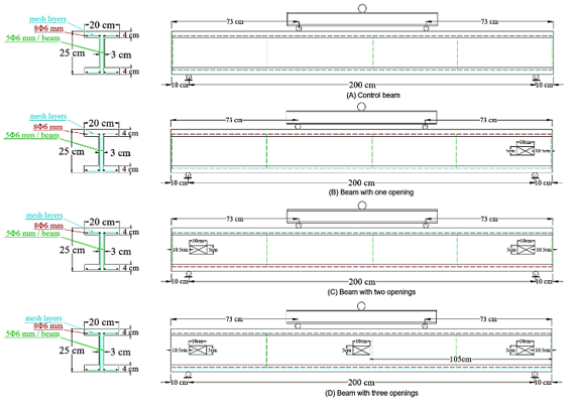


**Figure 2: Dimensions of the tested beams and the openings.**

(A) Beams reinforced with welded metal mesh.

(B) Beams reinforced with tensar mesh.

**Figure 3: The shape of the meshes used, during their preparation.**

### 3-Mortar Matrix

The ferrocement sand-cement mortar was made up of sand, blast furnace cement, silica fume, and fly ash. The main purpose of the mix design was to determine how the high amount of cement could be partially replaced by silica fume and fly ash to increase the strength of the mortar matrix with no detrimental effects on the quality and properties of the mix in both the fresh and hardened states. To allow the mortar matrix to penetrate through the layers of steel mesh reinforcement, sufficient workability was required. To increase flow characteristics and accelerate the early strength development, a super plasticizing agent was utilized. The ferrocement mortar mixture had a water/cement ratio of 0.35, a super-plasticizer of 2% by weight of cement, a sand/cement ratio of 2.0, 10% by weight of cement was replaced by S.F and 20% by weight of cement was replaced by fly ash, with a percentage of addition of fiber e300 of 0.9 kg/m$^3$. After 28 days, the ferrocement mortar's average compressive strength ( $fcu$ ) was found to be 35 MPa. In the laboratory, a mechanical mixer with a capacity of 0.05 m$^3$ was utilized for all mixes where the volume of the combined ingredients was found to be within this range. First, the constituent materials were drying mixed, then the blended water was added and the entire patch was re-blended in the mixer. All beams were mechanically compacted.

### 4-Casting and Curing

The molds were prepared as I section. Contras wood was used to make the I-section mold. The shape of the I-beam molds is shown in figure (4). I-sections are characterized by the possibility of resisting large bending moments due to their large moment of inertia compared to the cross-section area. Therefore, these sections are used in many construction applications such as railway tracks etc. Of course, the authors do not mean I-section is the best nor has great advantages over other sections. Rather, it was studied in the current research as one of the common sections used in the field of construction.

**Figure 4: The shape of the I-beam mold.**

The mesh was then added to the mold after the foam was placed in the opening locations. Mixing and casting were done. The mixing procedure was the same for all concrete mixes. Fine aggregate and cement were mixed dry first, and then 50 percent of the required water was added. The remaining 50% of the needed water with the admixture was then progressively added. The overall mixing time was around 10 minutes, which was sufficient to produce a homogenous mixture. Finally, beams were placed in the forms for 24 hours in laboratory conditions until the sides of the forms were stripped away, and then the beams were cured with wet burlap as shown in figure(5).

**Figure 5: Curing of the beams with wet burlap.**

**5-Tests Setup and Instrumentation**

The beams were painted with white paints after 28 days to aid in crack detection during the testing process. As illustrated in figure (6), four demec points were positioned on the upper and lower flange in the mid-span of the beam on one side of it to measure the strain versus load during the test.

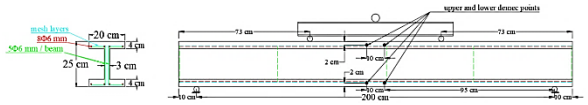


**Figure 6: Locations of the demec points on the tested beams.**

All specimens were tested on the testing loading frame. The test was carried out under a four-point loading system. The specimen was centered on the test setup, with a constant spread of 2000mm between the two supports. The applied loads' distance is 73 cm apart from both ends of the beam. Two dial gauges were fixed at the upper and lower demec points. A hydraulic jack with a maximum capacity of 80.0 kN was used to increase the load every 5 kN, as shown in figure (7).

**Figure 7: Beam under loading.**

The strain values were estimated by multiplying the readings by the gauge factor of the mechanical gauge employed while the beam deflection was determined by recording the dial gauge readings at each load increment. Figure (8) shows the dial gauge and the deflection gauge used. Throughout the specimen's side, cracks were traced and marked. Each specimen's initial crack load, crack propagation, and failure mode were all recorded. The load on the sample was increased until the fracture.

a) Dial gauge b) Strain gauge

**Figure 8: The dial gauge and the deflection gauge used.**

**6-Test Results and Discussions**

**6-1 First crack loads and ultimate loads**

The obtained results for the first cracking load, ultimate load, ductility ratio, and energy absorption are shown in Table 3.

**Table 3: Experimental results of the structural behavior of tested beams.**

| Group No. | Code of beams | Pc (kN) | U.l. (kN) | 1st crack Def. (mm) | Max. Def. (mm) | Ductility Ratio | Energy Absorb. (kN.mm) | U.l./weight (kg/kg) |
|---|---|---|---|---|---|---|---|---|
| A | W0 | 11.2 | 45.1 | 1.11 | 12.5 | 11.3 | 303 | 55.1 |
| | W1 | 10.2 | 41.3 | 1.08 | 10.9 | 10.3 | 239 | 50.5 |
| | W2 | 9.7 | 38.0 | 1.04 | 9.74 | 9.4 | 197 | 46.7 |
| | W3 | 9.0 | 35.4 | 1.04 | 9 | 8.64 | 169 | 43.6 |
| B | T0 | 11.0 | 37.0 | 1.22 | 6.75 | 5.51 | 129 | 45.1 |
| | T1 | 10.7 | 36.2 | 1.21 | 6.64 | 5.48 | 126 | 44.3 |
| | T2 | 13.1 | 34.5 | 0.78 | 5.81 | 7.48 | 122 | 42.4 |
| | T3 | 12.6 | 33.6 | 0.76 | 5.68 | 7.48 | 118 | 41.4 |

During the test, the cracking load, the ultimate load, the deflection at the first cracking load, and the deflection at the ultimate load were measured and obtained, while the ductility ratio and energy absorption for each tested beam was calculated from the load versus deflection diagram. Figure (9) shows the first cracking load and ultimate load values for all of the tested beams.

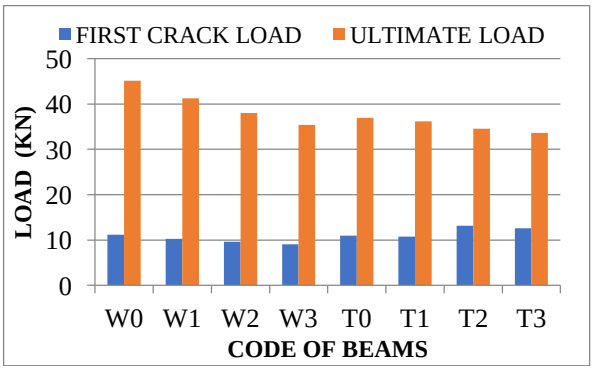


**Figure 9: First crack load and ultimate load of all tested beams.**

As shown in figure, W0 obtained a maximum ultimate load of 45.1 kN while T3 obtained a minimum ultimate load of 33.6 kN. Beams with welded steel meshes show a higher ultimate load than beams with tensar meshes type SS40 by 22%, 14%, 10%, and 5.4% for beams without opening, one, two, and three openings, respectively. This may be related to the differences between the properties of used meshes where, at a constant reinforcing ratio, welded steel meshes as a metallic mesh had higher properties, which improved the performance of the beams than beams reinforced with tensar meshes as a non-metallic mesh.

**6-2 Ductility Ratio**

The ductility ratio is defined as the ratio of the mid-span deflection at ultimate load to that at the first crack load($\Delta u/\Delta y$). Welded steel mesh beams show a greater ductility ratio than tensar mesh beams. Figure (10) shows ductility ratios for all tested beams.

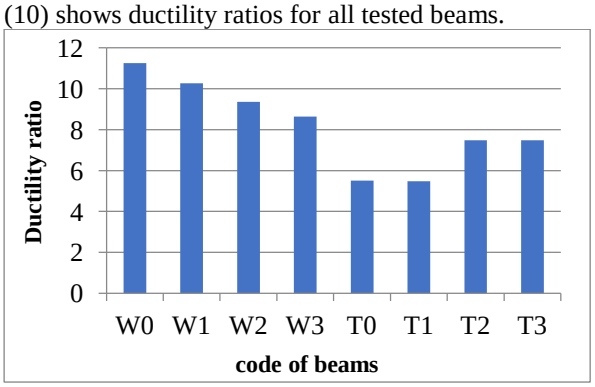


**Figure 10: Ductility Ratio of all tested beams.**

As shown in figure, beams reinforced with welded metal mesh have higher ductility ration compared to those reinforced with tensat. This may be related to the higher maximum deflection values of welded beams than the maximum deflection of tensar beams while the deflection at first crack loads of welded beams is close to the deflection at first crack loads of tensar beams.

**6-3 Energy Absorption**

The area beneath the load-deflection curve is referred to as energy absorption. The area under the curve was calculated using a computer program (BASIC language) by integrating the equation of the load-deflection curve for each beam specimen as follows:

Ultimate load absorbed energy = $\int f(\Delta)\, d\Delta$ (Eq. 1)

Where $f(\Delta)$ is the load defection curve equation and u is the mid defection at failure load. The energy absorption of beams reinforced with welded steel mesh was higher than beams reinforced with tensar mesh. The energy absorption of all measured beams is highlighted in figure (11).

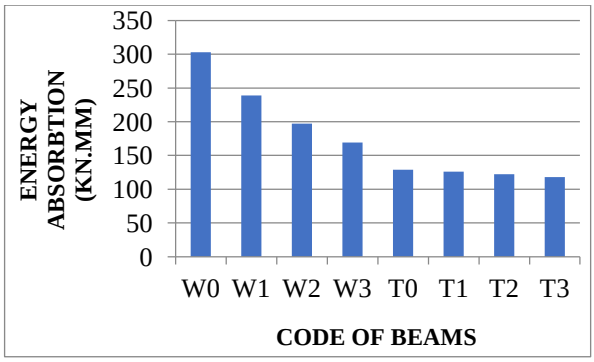


**Figure 11: Energy absorption of all tested beams.**

**6-4 Load versus deflection relationship**

The relationship between the applied load and the central deflection for the tested beams is presented in figures (12) to (14).

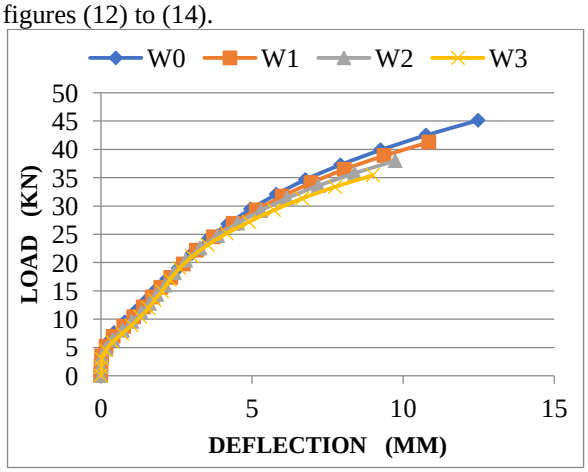


**Figure 12: Load versus deflection curves of the group (A).**

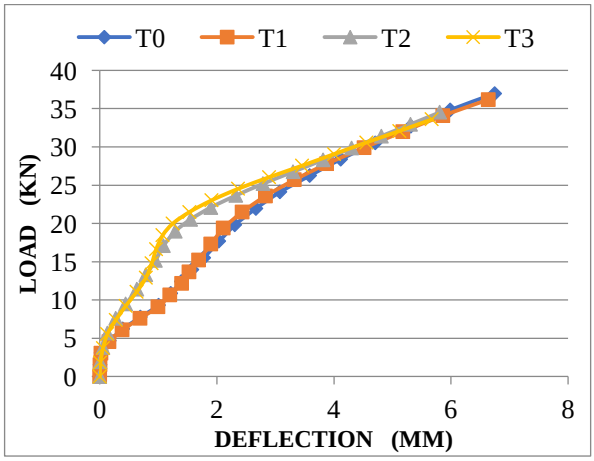


**Figure 13: Load versus deflection curves of the group (B).**

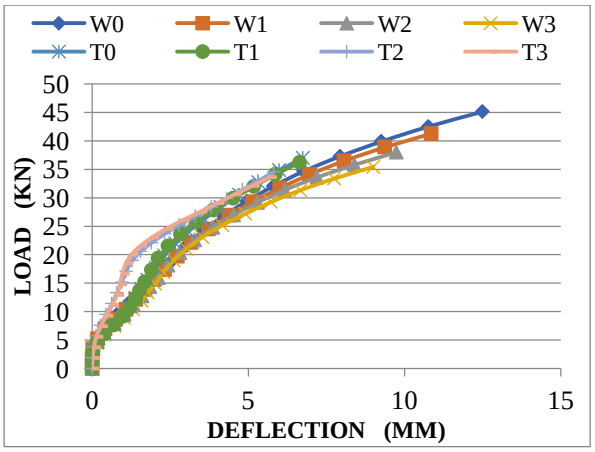


**Figure 14: Load versus deflection curves of all tested beams.**

The load-deflection relationship for the group (A) was nearly linear up to around 11.15 kN, 10.23 kN, 9.65 kN, and 9.04 kN for beams W0, W1, W2, and W3, respectively, when the divergence from the linear relationship began. As shown in figure (12), the maximum deflection for beams W0, W1, W2, and W3 was 12.5 mm, 10.9 mm, 9.74 mm, and 9 mm, respectively.

The load-deflection relationship for the group (B) was nearly linear up to about 10.96 kN, 10.74 kN, 13.13 kN, and 12.58 kN for beams T0, T1, T2, and T3, respectively, when the deviations from the linear relationship began. The maximum deflection for beams T0, T1, T2, and T3 was 6.75 mm, 6.64 mm, 5.81 mm, and 5.68 mm, respectively, as shown in figure (13). As a possible explanation, in beams T0 and T1, the failure was due to bending which means higher bending moment values that cause the higher deflection values while at the same load, beams T2 and T3 obtained lower deflection values because some of the stresses go around the openings in shear zone and the remained stresses distributed in bending zone which causes the lowest deflection values.

As shown in figure (14), beams with welded steel meshes have higher load and deflection values compared to beams with tensar meshes. The ultimate load and maximum deflection for beams with welded steel meshes and beams with tensar meshes decreased as the number of openings increased. When compared to beams T0, T1, T2, and T3, the ultimate load for beams W0, W1, W2, and W3 increased by 22%, 14%, 10%, and 5.4 percent, respectively. In addition, as compared to beams T0, T1, T2, and T3, the deflection of W0, W1, W2, and W3 increased by 85.1 %, 63.4%, 67.6 %, and 58.5%, respectively.

**6-5 Compressive and Tensile Strain**

Figures (15) and (16) show the load versus strain curves for all tested beams. The relationship between load and strain was practically linear up to the first cracking load, after which it began to depart from the linear relationship.

For group (A), the compressive strain increased with the increase of the applied load as shown in figure (15). For beams W0, W1, W2, and W3 the maximum compressive strain reached about -0.0048, -0.0039, -0.0032, and -0.0026 respectively at maximum load 45.11 kN, 41.25 kN, 37.98 kN, and 35.42 kN. However, the maximum tensile strain for beams W0, W1, W2, and W3 was 0.0425, 0.0348, 0.0283, and 0.0234 respectively at a maximum load of 45.11 kN, 41.25 kN, 37.98 kN, and 35.42 kN. As a possible explanation, it can be said that the behavior of the load-strain curve consisted of three main zones, which are the uncracked zone, cracking zone, and cracks propagation zone. In the uncracked zone, from zero loads to the first crack load there is no crack, which makes the strain values approximately equal to zero. Then in the cracking zone, there was a linear relationship between loads and strain, which caused an increase in strain values with the increased loads due to cracks. Finally, the cracks propagation zone consisted of two zones where, the first zone had lower strain values with the applied loads because the majority of the stresses were resisted by the meshes while, in the second zone, the beams showed the highest strain values with the increased loads as a result of the propagation of cracks.

For group (B), the compressive strain increased with the increase of the applied load as shown in figure (16). For beams T0, T1, T2, and T3 the maximum compressive strain reached about -0.0018, -0.0016, -0.0012, and -0.0011 respectively at maximum load 36.97 kN, 36.19 kN, 34.52 kN, and 33.6 kN. However, the max tensile strain for beams T0, T1, T2, and T3 was 0.0165, 0.0146, 0.0102, and 0.0098 respectively at a maximum load of 36.97 kN, 36.19 kN, 34.52 kN, and 33.6 kN. As a possible explanation, it can be said that, for beams T0 and T1, the first cracks were due to bending which makes the first crack load lower than of first crack load of beam T2 and T3 in which the cracks was combined between bending cracks and shear cracks due to the increasing number of openings, especially in shear zones which makes the stresses concentrated around the openings in shear zones which cause an increase in first crack load due to the higher strength of tensar meshes in shear. For example at a load of 16 tons, for T0 and T1, the majority of stresses were concentrated in the bending zone at the mid-span of the beams while the measurement of the strain was at the mid-span of the beams therefore, beams T0 and T1 obtained higher strain values. In contrast, in beams T2 and T3, there were more openings, which make some of the stresses go around the openings in shear zones while, the remained stresses were distributed at the bending zone at mid-span, which cause the lower strain values.

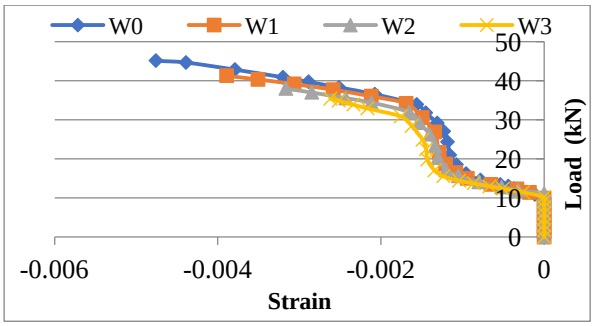


**(a) Load vs. compressive strain.**

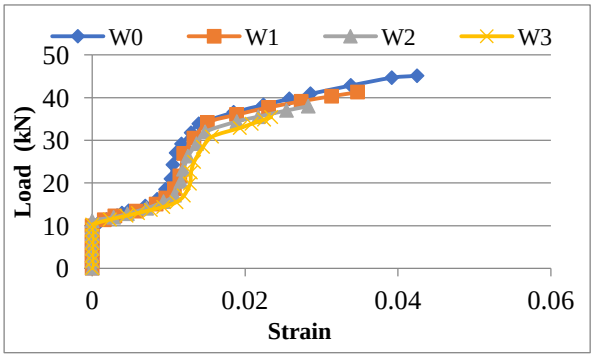


**(b) Load vs. tensile strain.**

**Figure 15 (a and b): Load versus strain Curves of the group (A).**

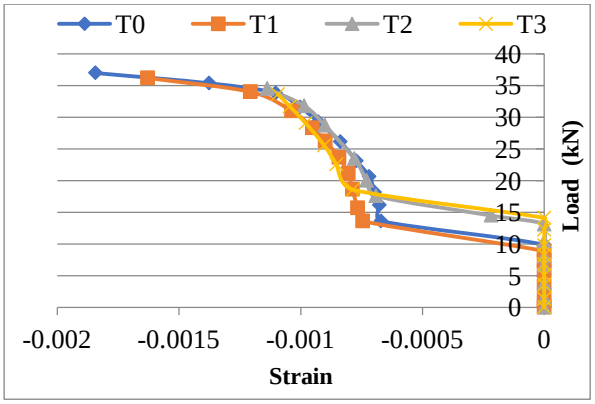


**(a) Load vs. compressive strain.**

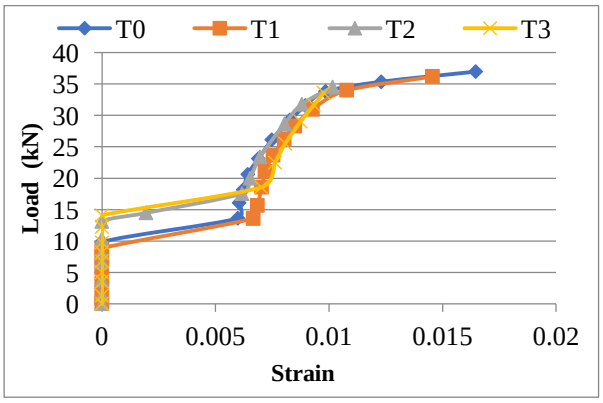


**(b) Load vs. tensile strain.**

**Figure 16 (a and b): Load versus strain curves of the group (B).**

### 6-6 Load-to-weight ratio

To obtain how the number of openings affects the behavior of ferrocement beams, the load-to-weight ratio was calculated. The load-to-weight ratio is defined as the ratio between the ultimate load and the weight of the beams. The load-to-weight ratio values are shown in Table 3. The load-to-weight ratio for all tested beams was drawn as shown in figure (17). As shown in figure (17), it can be said that, as the number of openings increases, the load-to-weight ratio decreases. The effect of placing three openings in beams with the dimension of 10 x 5 cm reduced the load-to-weight ratio by 20.7% and 8.2% compared to the beams with no openings for welded beams and tensar beams respectively.

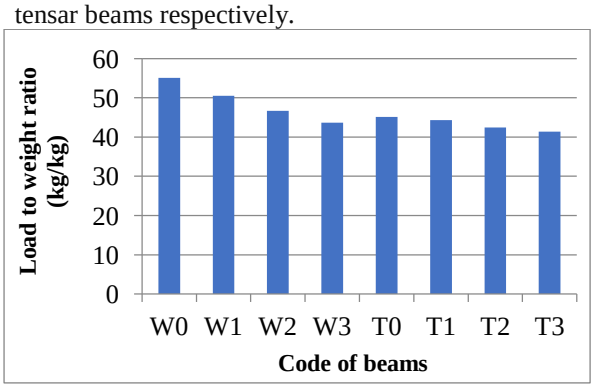


**Figure 17: Load to weight ratio of all tested beams.**

### 6-7 Effect of Openings on the Performance of tested Beams

The ultimate load in beams with three openings decreased by 21.5% compared with the ultimate load in beams with no openings for welded steel mesh beams, while the ultimate load in beams with three openings decreased by 9.1% compared with the ultimate load in beams with no openings for tensar mesh beams. The maximum deflection of the welded beam with three openings decreased by 28% compared with the maximum deflection of the welded beam with no opening while the maximum deflection of the tensar beam with three openings decreased by 15.9% compared with the maximum deflection of the tensar beam with no opening. The ductility ratio of the welded beam with three openings decreased by 23.3% compared with the ductility ratio of the welded beam with no opening while the ductility ratio of the tensar beam with three openings decreased by 35.8% compared with the ductility ratio of the tensar beam with no opening. The effect of placing three openings in beams with the dimension of 10 x 5 cm reduced the load-to-weight ratio by 20.7% and 8.2% compared to the beams with no openings for welded beams and tensar beams respectively.

### 6-8 Cracking Patterns and Mode of Failure

Cracks were traced and marked over the beam's side. Each beam's first crack load, crack propagation, and failure mode were all recorded. Flexural cracks appeared towards the beam's mid-span. The cracks progressed vertically as the load increased, and new

flexural cracks appeared quickly. When the specimens approached their failure load, the cracks began to propagate wider. As the load increased, more cracks appeared, and the crack at mid-span began to spread vertically towards the beam's top surface, whereas the majority of the generated cracks did not. This could be attributed to the effect of steel mesh in controlling the crack width. The cracks for all tested beams can be shown in figure (18). As shown in figure (18), the cracking patterns and mode of failure for all welded tensar beams with openings seem to be combined between shear and bending failure but the greatest effect was due to bending.

**(a) Beams of the group (A) with welded mesh.**

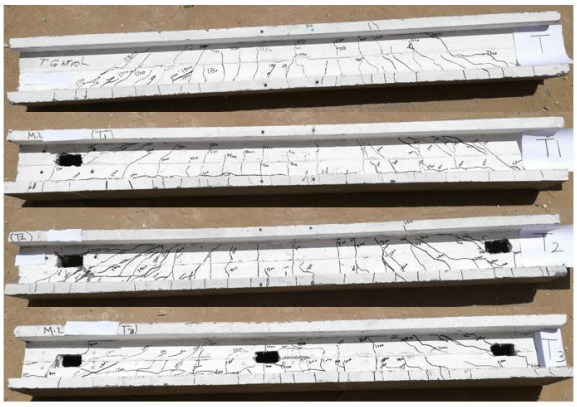

**(b) Beams of the group (B) with tensar mesh.**

**Figure 18 (a and b): Cracking patterns of all tested beams.**

## 7-CONCLUSIONS

The current studies the effect of web openings on the structural behavior of ferrocement I-beams reinforced with metallic and non-metallic meshes. Therefore, eight ferrocement I-beams are cast, cured, and tested under a four-point loading system. The eight beams are divided into two groups. The first group contains four beams with no opening, one, two, and three openings that are reinforced with welded steel mesh as a metallic mesh while, the other group contains four beams with no opening, one, two, and three openings that are reinforced with tensar mesh type SS40 as a non-metallic mesh. To keep a constant reinforcement ratio, the two groups are, respectively, reinforced with three layers of welded steel meshes and two layers of tensar meshes.

Based on the experimentally available results, the following conclusions are drawn:

1. The number of openings has a substantial effect on the behavior of tested beams in which as the number of openings increases, the ultimate load, the maximum deflection, and the load-to-weight ratio decrease.
2. Placing three openings in beams with the dimension of 10×5 cm reduced the load-to-weight ratio by 20.7% and 8.2% compared to the beams with no openings for welded beams and tensar beams, respectively.
3. For all tested beams: with no opening, one, two, and three openings, beams with welded steel meshes had a greater ultimate load than beams with tensar meshes by 22%, 14%, 10%, and 5.4 %, respectively.
4. Beams with welded steel meshes had a higher deflection than beams with tensar meshes by 85.1%, 63.4%, 67.6%, and 58.5% for beams without opening, one, two, and three openings, respectively.
5. Beams with welded steel meshes (as a metallic mesh) had a greater ductility ratio and energy absorption than beams with tensar meshes (as a non-metallic) with a constant reinforcing ratio.
6. Beams with welded steel meshes (as a metallic mesh) had higher compressive and tensile strains than beams with tensar meshes (as non-metallic) with a constant reinforcing ratio.

## REFERENCES


[1] ACI 549R-97, "State-of-the-Art Report on Ferrocement", Manual of Concrete Practice, ACI Committee 549, Farmington Hills, Michigan, 1997.

[2] ACI 5492R-04, "Report on Thin Reinforced Cementitious Products", Farmington Hills, Michigan, ACI Committee 5492R, 2004.

[3] Ankit B., Sumit G., Lalit K., Hardik S., "**A Review Study of Application of Ferrocement**", International Research Journal of Engineering and Technology (IRJET), V. 04, Issue 06, June - 2017, pp. 1592-1597.

[4] Shaheen Y.B.I., Soliman N.M., and Hafiz A.M., "**Structural Behavior of Ferrocement Channels Beams**". Concrete Research Letters, V. 4, No.3, 2013, pp. 621-638.

[5] Shaheen Y.B.I., and Swamy R.N., "**Tensile Behavior of thin Ferrocement Plates**". Special Publication, 124, 1990, pp.357-388.

[6] Kandil, D.E.M., "**Impact Resistance of Reinforced Ferrocement Concrete Plates**". M. Sc. Thesis submitted to Menoufia University, Egypt, 2013.

[7] Shaheen Y.B.I., Mohamed A.M., and Mohamed, H.R., "**Structural Performance of Ribbed Ferrocement Plates Reinforced with Composite Materials**", Struct. Eng. Mech., V.

60, No. 4, 2016, pp. 567-594.

[8] Shaheen Y.B.I., and Eltehawy E.A., "**Structural Behaviour of Ferrocement Channels Slabs for Low-Cost Housing**". Challenge J. Concr. Res. Lett, V. 8, No. 2, 2017, pp. 48-64.

[9] Shaheen Y.B.I., Mousa M, and Gamal E., "**Structural Behavior of Light Weight Ferrocement Walls**", 13th International Conference on Civil and Architecture Engineering. Cairo, Egypt, 2020, pp.1-21.

[10] Shaaban I.G., Shaheen Y.B.I., Elsayed E.L., Kamal O.A., and Adesina P.A., "**Flexural Behaviour and Theoretical Prediction of Lightweight Ferrocement Composite Beams**", Case studies in construction materials, V. 9, 2018, e00204.

[11] Naaman, A.E., **"Ferrocement and Laminated Cementitious Composites",** Ann Arbor, Michigan, USA, Techno-Press 3000, 2000, p. 26, ISBN 0-9674030-0-0.

[12] Sumadi S., and Ramli M., **"Development of Lightweight Ferrocement Sandwich Panels for Modular Housing and Industrialized Building System"**, Project Report, University Teknologi Malaysia (UTM), Research Vote 73311, 2008.

[13] International Ferrocement Society, "**Ferrocement Model Code**", Thailand, IFS, 2001.

[14] Onet T., Magureanu C., and Vescan V., "**Aspects Concerning the Behavior of Ferrocement in Flexure**", Journal of Ferrocement, V. 22, No.1, 1992, PP. 1-9

[15] Suksawang N., Nassif H.H., and Sanders M., **"Analysis of Ferrocement- Laminated Concrete Beams"**, Proceedings of Eighth International Symposium and Workshop on Ferrocement and Thin Reinforced Cement Composites, Bangkok Thailand, IFS, 06-08 February 2006, PP. 141-150.

[16] Mansur M.A., and Ong K.G.C., "S**hear Strength of Ferrocement Beams**", ACI Structural Journal, Vol. 84, No.1, 1987, pp. 10-17.

[17] Al-Rifai W.N., "**Ferrocement Wall: Penetration Testing, Proceedings of Eighth International Symposium and Workshop on Ferrocement and Thin Reinforced Cement Composites"**, 06-08 February 2000, Bangkok Thailand, IFS, pp. 177-185.

[18] Fouad E.A., John N. M., and Charles K. K., **"Openings Effect on the Performance of Reinforced Concrete Beams Loaded in Bending and Shear**", Engineering, Technology, and Applied Science Research, Vol. 10, No. 2, 2020, pp. 5352-5360.

[19] Acma L., and Mariano C., "**Development and Application of Ferrocement I-beams"**, Doctor of Engineering Dissertation, Philippines: MSU-IIT, Iligan City, 2014.

[20] E.S.S.1109/2008, "**Aggregates for Concrete**", Ministry of Industry, Cairo, Egypt, 2008.

[21] E.S.S.4756/2013, "**Testing the Physical and Mechanical Properties of Cement**", Ministry of Industry, Cairo, Egypt, 2013.

[22] Shaheen Y.B.I., Zeinab A.E., and Aya M.E., "**The Flexural Behavior of Ferrocement Composite Hollow-Cored Sections**", Journal of Engineering Research and Reports, V. 20, No. 12, Aug. 2021, pp. 26-41, Article no. JERR.73276, ISSN: 2582-2926.

[23] Tensar International (2001a), "**The Properties and Performance of Tensar Biaxial Geogrid**", Technical Publications, 2.